

Received 18 December 2023, accepted 31 December 2023, date of publication 5 January 2024,
date of current version 11 January 2024.

Digital Object Identifier 10.1109/ACCESS.2024.3350204

RESEARCH ARTICLE

Lyapunov Based Nonlinear Model Predictive Control of Wind Power Generation System With External Disturbances

JINMAN LUO¹, YUQING LI¹, PIAO LIU¹, SIQI YE¹, RUIJUE FENG², AND JINYANG WANG^{2,3}

¹Dongguan Power Supply Bureau of Guangdong Power Grid Corporation, Dongguan 523000, China

²College of Electrical Engineering, Guangzhou City University of Technology, Guangzhou 510800, China

³College of Electric Power, South China University of Technology, Guangzhou 510006, China

Corresponding author: Piao Liu (2581133079@qq.com)


ABSTRACT Wind energy has been promoted as an environmentally-friendly and sustainable energy. The boost of wind power generation has greatly promoted the developments of modern urbanization. However, the characteristics of complexity, nonlinearity, constraints and multivariability make the controller design challenging. In this work, a Lyapunov-based MPC framework is proposed for nonlinear wind power systems with external disturbances and constraints. Firstly, a typical doubly-fed wind power generation system is established in line with the physical models of key components, i.e., wind turbine, transformation device and generator. Then, considering the exogenous disturbances, a nonlinear Lyapunov-based MPC framework is proposed for the wind power generation system. The optimization objective and constraints are constructed to formulate the control problem. As well, the closed-loop stability of presented MPC approach is derived. In the end, an actual 5MW wind power system is utilized to verify and analyze the effectiveness of designed controller under different wind speeds and weighting parameters.

INDEX TERMS Wind power generation system, model predictive control, nonlinear controller, Lyapunov function.

I. INTRODUCTION

Increasing urbanization has aggravated the contradiction in global energy supply and demand. Seeing that the severe pollution and source shortage in fossil fuels, it is urgent to explore renewable energy, where wind energy stands out for its green, clean and sustainable nature [1], [2]. For one thing, in contrast to traditional sources, wind energy is environmentally friendly instead of producing harmful gases or pollutants. For another, excellent economic advantages are performed in the utilization of wind power, since the plants spend lower costs in operation and shorter time in construction. Hence, wind power generation, converting wind energy to electric power, has become a key choice in modern development [3]. Nevertheless, the control problem

in wind power systems is still a challenging issue for their characteristics of nonlinearity and hard constraints [4]. More attention must be paid to the research on their optimization strategies certainly [5]. A wind power system consists of rotor, transmission system, tower, and generator. During the conversion in work, the energy has gone from wind source, to mechanical energy, and finally to electric power. When the wind speed reaches a certain range, the blades are propelled, and then drive the rotor, connected with the transmission system, to produce electricity in the generator [6]. The control part plays a crucial role in the wind power system, in charge of the start-up, grid connection, power generation and so on, to guarantee a safe and efficient operation. However, due to the characteristics of randomness and intermittency, it is difficult to accurately predict the outputs of wind power generation. In particular, the curtailment of electric power occurs when the system is integrated into the grid. Further,

The associate editor coordinating the review of this manuscript and approving it for publication was Jorge Esteban Rodas Benítez .

noting that the fluctuation of wind inputs poses a threat to the stability of grid, the criticality of control design is underlined [7].

Model predictive control (MPC) technique was first proposed in the 1960s and found its initial applications in the field of chemical process control [8], [9], [10], [11]. For the past few years, MPC has been widely adopted in diverse fields [12], [13], [14], [15], [16], e.g., mechanical control, power systems, transportation and aviation. The fundamental idea of MPC is to perform multi-step predictions of system model within each control cycle and solve the optimization problem in line with the predictions. The optimization aims to obtain an input sequence that minimizes the objective function over the prediction horizon. Ultimately, only the first input in the sequence will be used to the actual system at the current time step. MPC is a model-based strategy applied to nonlinear power systems [7]. For wind power systems, MPC makes significant improvement in performance and stability, through dealing with the nonlinearity and stochastic disturbances effectively. As constructing predictive model and integrating optimization theory, it predicts the future actions and calculates the optimal control inputs. In addition, MPC operates within hard/soft constraints to ensure the system requirements. To this end, in wind power system, MPC technique provides a great assurance for its efficient and stable operations [18]. Now, the application of MPC has spawned many new technologies. For instance, a novel MPC approach was proposed by combining MPC with Sliding-Mode Control (SMC) to address system uncertainties in [19]. Moreover, by combining MPC with Takagi-Sugeno (T-S) fuzzy models (TSFMs), the implementation efficiency was improved for nonlinear systems in [20]. In [21], a novel cooperative H_∞ robust move blocking fuzzy MPC approach was proposed to compensate for model uncertainties and external disturbances while ensuring closed-loop stability.

To obtain controls with explicit stability, the use of Lyapunov method has attracted increasing attention. Closed-loop stability regions are well-defined by these rules. A class of Lyapunov-based nonlinear controller was developed in [22], [23], and [24], where explicit initial conditions were raised for bounded robust stability, and yet no performance was considered. Currently, a focus is Lyapunov-based MPC (LMPC) in various complicated systems such as robot systems [25], distributed systems [26] and intelligent systems. Besides, LMPC can be combined with other schemes (e.g., fuzzy control and adaptive control) to enhance performance and robustness. As the mentions, LMPC suggests the incorporation of MPC and Lyapunov stability theory. More specifically, in this approach, a Lyapunov function is constructed and introduced to the MPC framework to analyze the system stability [29]. In the framework, the Lyapunov function serves as an energy function for the assessment of system stability and states convergence. By selecting appropriate Lyapunov function, the stability and performance objectives can be satisfied under the designed control algorithm.

The challenges in dealing with wind power system lie in several aspects: 1) a wind power system is a complex nonlinear dynamic system, including multiple subsystems such as wind turbines, rotors, and generators, which are interconnected. It is not easy to control such system with linear control algorithm. Thus, a nonlinear Lyapunov MPC is designed for the wind power system. 2) For the wind power systems, wind speed is a critical influencing factor in the performance with highly randomness and not easy to measure. These uncertainties pose significant challenges to LMPC control. 3) LMPC needs to calculate the optimal control inputs in real-time, considering the dynamic changes in wind speed. It requires fast responses and adjustments due to the dynamic variation in wind speed. However, the process of calculating the optimal control inputs may have a high computational complexity, presenting a challenge to real-time responsiveness.

In the wind power generation, the goal is to capture as much wind energy as possible in low wind speed region, as well as maintain a rated output power in high wind speed region. It is supposed to design compatible control schemes at different work. Therefore, in our work, a Lyapunov-based MPC framework is proposed to address the control problem of disturbed wind power system. Both state and input constraints are fulfilled in LMPC design. Bounded controllers and corresponding stable regions are utilized as auxiliary controllers to complete the stability analysis.

The main contributions of our manuscript are:

- 1) A robust Lyapunov-based MPC approach is proposed for wind power system. The proposed Lyapunov-based MPC approach allows us to take into account the nonlinear nature of the system and external perturbations while maintaining stability. The difference between LMPC and regular MPC is that we incorporated constraints based on the Lyapunov function into the MPC in the optimization process.
- 2) Handling external perturbations is an important challenge in the control of wind power systems. The proposed approach combines Lyapunov control and nonlinear model predictions to provide robustness to external perturbations, which is an innovative approach.
- 3) Soft constraints are derived in the optimization process for the high wind speed phase, providing the system with a broader operating range to achieve stability more rapidly. The effectiveness of the proposed approach has been validated in an offshore wind power generation system.

The remainder of the paper is organized as follows. Section II presents the mathematical model of wind power generation system, which lays a foundation for controller design. In Section III, a Lyapunov-based nonlinear MPC is designed for the power generation system with external disturbances. Simulation experiments are given in Section IV to show the effectiveness of the proposed control framework. Finally, Section V concludes the main work of this paper.

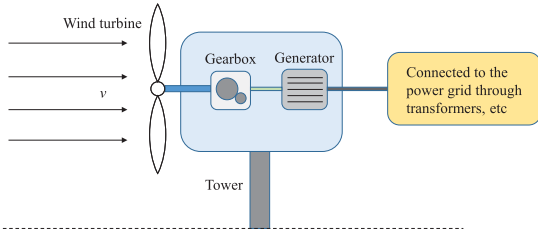


FIGURE 1. Composition of wind power generation system.

II. WIND POWER GENERATION SYSTEM MODELING
A. SYSTEM CONFIGURATION

As shown in FIGURE 1, in general, a large-scale wind power generation system is comprised of wind turbine, tower, transmission device, generator, inverter, control equipment and power grid [27]. The cooperation of each component facilitates the conversion from wind energy to electric power. Specifically, wind energy is captured by the wind turbine and transformed into mechanical energy. Then, the energy is transferred in the form of rotational speed and torque to the generator through the transmission device. The device matches the speed of wind turbine with the requirements of generator by virtue of a gearbox or direct drive system. As for the generator, it completes the transformation from mechanical energy into alternating current (AC) power on the basis of electromagnetic induction. In the end, the generated electric power is integrated into the power grid, in which AC power is converted to direct current (DC) power by the inverter, and the voltage level is adjusted by the transformer.

By controlling the inverter, the grid connection strategies are executed to guarantee the synchronization of wind power generation system and power grid, and maintain stable output power. For the sake of seamless connection and power regulation, the parameters of grid are monitored to modify the operating mode of inverter.

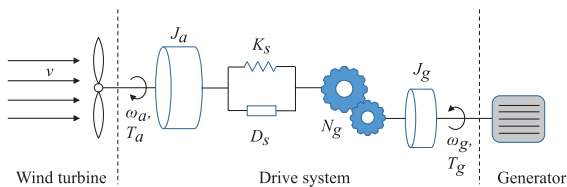


FIGURE 2. Simplified model of wind power generation system and its parameters.

It is intractable to address the nonlinearity and complexity of wind power generation system. Hence, in this paper, some simplifications have been introduced to better achieve the research objectives. The specific model and parameter symbols are illustrated in FIGURE 2. The components like inverter, controller and power grid are omitted for brevity. We have concentrated on modeling wind turbine, transmission system, and generator.

1) WIND TURBINE

Based on aerodynamics, the wind turbine make full used of wind energy by rotor blade. When the wind acts on the blade, there exists difference of air pressure between the upper and lower surfaces, by virtue of the blade’s specific airfoil shape and angle of attack, such that the lift is generated to drive the blade to rotate. This allows for the maximum conversion from wind energy to mechanical energy [28].

The captured wind energy by the wind turbine can be represented as the following equation:

$$P_v = \frac{1}{2} \rho \pi R^2 v^3 C_p(\lambda, \beta) \tag{1}$$

where v is the current wind speed; P_v is the aerodynamic power captured by the aerodynamic unit from the wind; ρ is the air density; R is the radius of the wind turbine rotor; λ and β respectively represent the tip speed ratio and pitch angle of the blades; $C_p(\lambda, \beta)$ are wind energy utilization coefficients related to λ and β .

Specifically, the relationship between the wind energy utilization coefficients C_p and λ, β can be expressed by the following equations:

$$C_p(\lambda, \beta) = 0.5176 \left(\frac{116}{\lambda_i} - 0.4\beta - 5 \right) e^{-\frac{21}{\lambda_i}} + 0.0068\lambda \tag{2}$$

$$\frac{1}{\lambda_i} = \frac{1}{\lambda + 0.08\beta} - \frac{0.035}{\beta^3 + 1} \tag{3}$$

$$\lambda = \frac{\omega_a R}{v} \tag{4}$$

where ω_a is the wind turbine rotor angular speed. It can be seen that C_p is a nonlinear function of λ and β . There exists a pair of λ and β values for which the wind energy utilization coefficient C_p can reach its maximum value $C_{p,max}$. At this optimal condition, the corresponding values of λ and β are defined as λ_{opt} and β_{opt} respectively, where λ_{opt} is also referred to the optimal tip speed ratio. The specific equation is as follows:

$$(\lambda_{opt}, \beta_{opt}) = \arg \max_{\lambda, \beta} C_p(\lambda, \beta) \tag{5}$$

According to (1), the aerodynamic power of the wind turbine P_v is directly proportional to the wind energy capture coefficient C_p , i.e., as C_p increases, P_v also grows proportionally. Therefore, the aim is to maximize the value of C_p and employ MPC algorithm to achieve on-line optimization. This implies that it is available to enhance performance and economic efficiency of wind power generation system.

Here we modeling the function C_p w.r.t. λ and β . It is observed that in 3-D space, there exists a maximum value of C_p at certain λ and β , as shown at the black point in FIGURE 3. At this point, C_p reaches approximately 0.48, λ is around 8.1 and β is equal to 0. Furthermore, from the 2-D plot of C_p against λ and β in FIGURE 4, it can be seen that each value of β corresponds to a curve, and each curve has a

peak. When $\beta = 0$, the curve has the highest peak compared with other β . Therefore, for the objective to maximize C_p , the values of λ_{opt} and β_{opt} are set as 8.1 and 0, respectively.

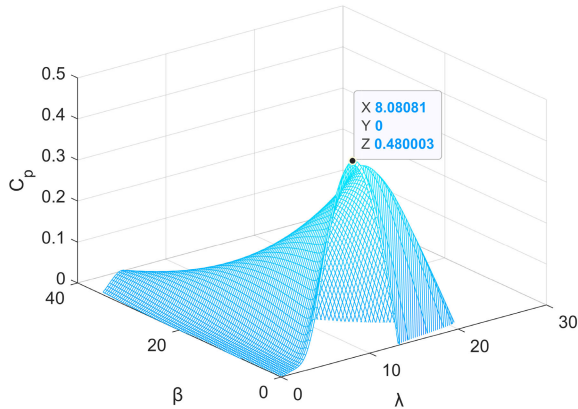


FIGURE 3. 3-D plot of C_p against λ and β .

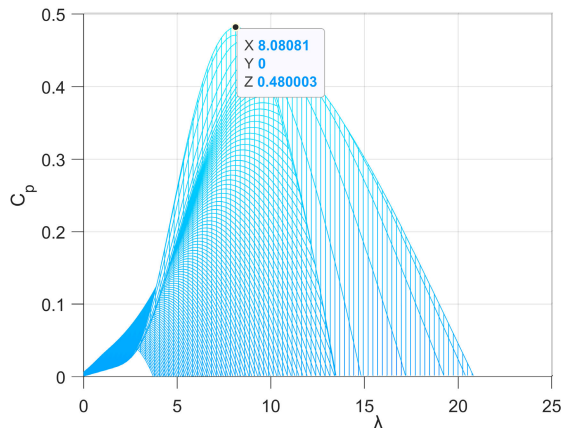


FIGURE 4. 2-D plot of C_p against λ under different β .

2) TRANSMISSION SYSTEM

As a crucial part of wind power apparatus, the transmission system is used to connect the low-speed shaft of wind turbine with the high-speed shaft of generator. It is composed of a series of transmission devices, e.g., wind turbine rotor, low-speed shaft, gearbox, and high-speed shaft. The rotor in wind turbine captures wind energy, and the low-speed shaft transfer the rotational force to the gearbox. Through the gearbox, the rotational speed is delivered across the high-speed shaft to prompt the electric power generation in generator. That is to say, the conversion from wind energy to mechanical energy is completed [28]. The types of shaft can be concluded with rigid shaft and flexible shaft. The rigid shaft, made of metal materials, is designed to transfer the rotational motion and bear the immense torque from wind turbine. On the other hand, the flexible shaft, made of high-strength elastic materials, enables to absorb the vibration, shock,

torque fluctuation and unbalanced load. The optimization about transmission system may strengthen the energy transfer efficiency and stability, reduce energy losses, and attenuate fatigue damage to shafts. This contributes to the reduction of maintenance cost and the advancement of reliability in wind power generation systems.

The transmission system can be modeled as the follow-up:

$$T_a = \frac{1}{2\omega_a} \rho \pi R^2 v^3 C_p(\lambda, \beta) = \frac{P_v}{\omega_a} \quad (6)$$

$$J_a \dot{\omega}_a = T_a - K_s \theta - D_s \dot{\theta} \quad (7)$$

$$J_g \dot{\omega}_g = \frac{K_s \theta}{N_g} + \frac{D_s \dot{\theta}}{N_g} - T_g \quad (8)$$

$$\dot{\theta} = \omega_a - \frac{\omega_g}{N_g} \quad (9)$$

where T_a , T_g represent the torque of wind turbine and generator, respectively; ω_g denotes the rotor angular velocity of generator; θ is the torsional angle of transmission shaft; N_g represents the gear ratio of gearbox; J_a and J_g respectively mean the wind turbine and generator inertia; K_s and D_s denote the stiffness and damping coefficient, respectively.

3) GENERATOR

The generator is an vital component in wind power generation. Following Faraday's law of electromagnetic induction, the current will be induced in coils when the rotor rotates and cuts through the magnetic field line. That is the realization of energy conversion. In our work, we prefer to model the widely-used doubly fed induction generator (DFIG), which is more efficient and flexible than the traditional one [2]. Thus bidirectional power flow takes place since both stator and rotor windings are connected to the grid. What's more, even if the grid fails, it allows DFIG to hold power regulation capability for the tunable brushless generator. Additionally, DFIG stands out in efficiency through the control of stator and rotor current to attain power and voltage regulation.

The research places importance on DFIG and model it mathematically in the two-phase synchronously rotating coordinate system. Accordingly, one has:

a) Voltage Equations:

$$\begin{cases} u_{sd} = R_s i_{sd} + p\varphi_{sd} + \omega_1 \varphi_{sq} \\ u_{sq} = R_s i_{sq} + p\varphi_{sq} + \omega_1 \varphi_{sd} \\ u_{rd} = R_r i_{rd} + p\varphi_{rd} + (\omega_1 - \omega_2) \varphi_{rq} \\ u_{rq} = R_r i_{rq} + p\varphi_{rq} + (\omega_1 - \omega_2) \varphi_{rd} \end{cases} \quad (10)$$

where u_s and u_r denote the stator and rotor voltages; i_s and i_r represent the stator and rotor currents; φ_s and φ_r are the stator and rotor magnetic flux; the subscripts d and q indicate their corresponding d-q coordinate axes, where d and q mean the d-axis and q-axis relative to the rotor's angular velocity difference, thus obviously $\omega_g = (\omega_1 - \omega_2)$.

b) Flux Linkage Equations:

$$\begin{cases} \varphi_{sd} = L_s i_{sd} + L_m i_{rd} \\ \varphi_{sq} = L_s i_{sq} + L_m i_{rq} \\ \varphi_{rd} = L_r i_{rd} + L_m i_{sd} \\ \varphi_{rq} = L_r i_{rq} + L_m i_{sq} \end{cases} \quad (11)$$

where L_m denotes the equivalent mutual inductance between stator and rotor; L_s and L_r are the stator and rotor equivalent self-inductance, respectively.

c) Electromagnetic Torque Equation:

$$T_g = N_p L_m (i_{sq} i_{rd} - i_{sd} i_{rq}) \quad (12)$$

where N_p is the number of pole pairs in DFIG.

d) Generator Output Power:

Taking energy losses into account, we define the efficiency of mechanical-to-electrical energy conversion as η . The output power of the generator P_g can be calculated using the following equation:

$$P_g = \eta T_g \omega_g \quad (13)$$

B. WIND SPEED MODEL

Wind energy, as an important clean energy source, originates from variations in atmospheric airflow and interactions within the climate system, and thus presents strong uncertainty. Hence, the modeling about wind speed is of great significance to control implementation.

Probability distribution function has common application during the modeling. In this case, the wind speed is decomposed into two components: mean wind speed and turbulent wind speed, to better describe the variability. The mean wind speed refers to the average value over long-term observation and is typically to do with season, geographical location, climate conditions, etc. It possesses such slow variation that it can be determined long-term statistical analysis. Nevertheless, the turbulent wind speed represents the fluctuating part of wind speed within a shorter time interval, which is posed for the complicated meteorology and the instable airflow. Intense variation takes place among the turbulent wind speed, and it can be characterized through instantaneous wind speed peaks, changes in wind direction and so on.

In this paper, for the sake of simplicity, only the magnitude of wind speed is considered, whereas the direction and other effects are disregarded. The mean wind speed is described via step function, and the turbulent wind speed v_r is concerned through Gaussian distribution. To impose restrictions on the random disturbance values, the turbulent wind speed is generated under a truncated Gaussian distribution:

a) Set the truncation range, i.e., the upper bound v_b of the absolute value of turbulent wind speed v_r . Given mean value μ and standard deviation σ , the probability density function $v_r \sim N(\mu, \sigma^2)$ is attained by:

$$f(x) = \frac{1}{\sigma\sqrt{2\pi}} e^{-\frac{1}{2}\left(\frac{x-\mu}{\sigma}\right)^2} \quad (14)$$

b) Generate a random number using the Gaussian distribution provided in step a).

c) If the random number generated in step b) falls within the truncation range, return the random number. If not, repeat step b) until a random number is within the truncation range.

C. OVERALL STATE SPACE EQUATIONS

Based on the modeling of each component in foregoing description, a simplified state-space model is built for subsequent control design. Denote the state variables as $x = [x_1 \ x_2 \ x_3]^T = [\omega_g \ \omega_a \ \theta]^T$; the input variables as $u = [u_1 \ u_2]^T = [\beta \ T_g]^T$; the outputs as $y = [y_1 \ y_2]^T = [P_g \ \omega_g]^T$. The state equations of simplified wind power generation system are defined as follows:

$$\begin{aligned} \dot{x}(t) &= f(x(t), u(t), v(t)) \\ y(t) &= h(x(t), u(t)) \end{aligned} \quad (15)$$

where:

$$\begin{aligned} f(x(t), u(t), v(t)) &= \begin{bmatrix} -\frac{B_\theta}{N_g^2 J_g} x_1 + \frac{B_\theta}{N_g J_g} x_2 + \frac{K_\theta}{N_g J_g} x_3 - \frac{1}{J_g} u_2 \\ \frac{B_\theta}{N_g J_a} x_1 - \frac{B_\theta}{J_a} x_2 - \frac{K_\theta}{J_a} x_3 + \frac{1}{J_a} T_a(u_1, v, x_2) \\ x_2 - \frac{1}{N_g} x_1 \end{bmatrix} \end{aligned} \quad (16)$$

$$\begin{aligned} h(x(t), u(t)) &= [\eta x_1 u_2 \ x_1]^T \end{aligned} \quad (17)$$

This section provides a detailed introduction of the wind power generation system, and establishes the mathematical models for wind turbine, transmission system and generator, respectively. Via the synthesis and analysis, the state equations of simplified wind power generation system are proposed to lay foundation for optimization.

III. LYAPUNOV-BASED MPC DESIGN FOR WIND POWER GENERATION SYSTEM

A. CONTROL OBJECTIVES

The drastic fluctuations in wind speed have tremendous impacts on wind power generation system. Therefore, to ensure the safe operation, it is necessary to formulate different control objectives under high/low wind speed [28]. For this purpose, the parameters, like rated wind speed and rated power, should be monitored to switch the control strategy in time and protect the system.

When the wind speed falls within the rated wind speed range, the control objective is to achieve maximum power output and further attain optimal power generation efficiency. However, when the wind speed surpasses the rated threshold, it must impose some strategies, for example adjusting the angle of blades, to prevent excessive load operation and safeguard the system. On the contrary, if the wind speed falls below the rated threshold, it should activate auxiliary generators or alternative power sources to keep operation from shutdown.

In FIGURE 5, where the wind speed is within different regions, the control objectives have been depicted. When the wind speed is below the cut-in wind speed v_{in} , the auxiliary generator is activated to ensure power supply at low level. When the wind speed reaches v_{in} , normal operation begins. At this point, it is supposed to optimize the generator torque T_g to maximize C_p and the output power. Thus the interval $v_{in} \sim v_{rated}$ is named as maximum wind energy capture region. When the wind speed v is in $v_{mid} \leq v < v_{rated}$, i.e., the transition region, the rated generator speed ω_{rated} can be reached, whereas the output power cannot reach the rated value. Hence, the goal is to maintain the speed ω_{rated} and maximize the output power. Further, when the wind speed reaches v_{rated} , each state should be sustained at rated value. For example, if the wind speed grows, the pitch angle β should be adjusted to reduce C_p for rated P_g and ω_g . Note that define such interval $v_{rated} \sim v_{off}$ as the constant power region. In the end, when $v > v_{off}$, the system shuts down.

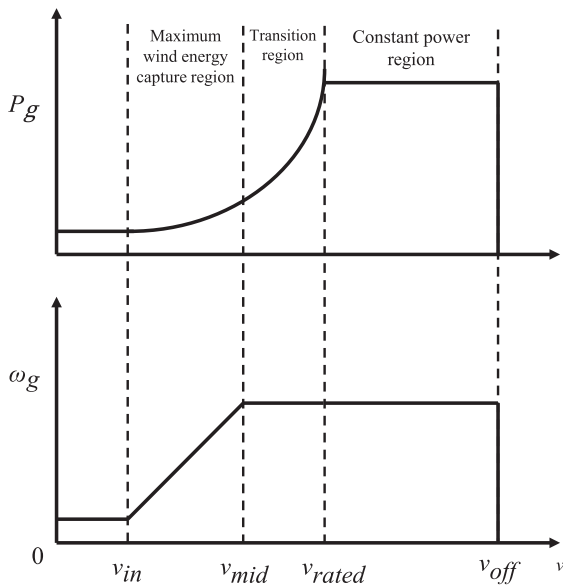


FIGURE 5. Control objectives at different wind speed regions.

In the above analysis, if the wind speed is within the maximum wind energy capture region, the control is designed to maximize the value of C_p equivalent to the maximum output power. A common solution is the optimal tip speed ratio method [28]. On the basis of blade design and control parameters of wind turbine, both performance and energy capture are achieved.

B. SYSTEM CONSTRAINTS

In actual wind power generation systems, it is inevitable to take the physical constraints into consideration. If not, the system may violate the restrictions, leading to the reduced lifespan of equipment and even operation accidents. Therefore, in optimization control, it is indispensable to impose constraints on variables to ensure the stability and security.

Generally, the constraints on wind power generation system include the limitations on wind turbine rotational speed, generator power output and the maximum torque of the transmission system. By taking these into account, the control algorithm can be optimized to ensure the safe, reliable and efficient operation to some extent.

Consider the constraints on state variables as $x \in \mathbb{X} \subseteq \mathbb{R}^{n_x}$, which can be formulated in detail as follows:

$$\begin{bmatrix} \omega_{g,\min} \\ \omega_{a,\min} \\ \theta_{\min} \end{bmatrix} \leq \begin{bmatrix} \omega_g \\ \omega_a \\ \theta \end{bmatrix} \leq \begin{bmatrix} \omega_{g,\text{rated}} \\ \omega_{a,\text{rated}} \\ \theta_{\max} \end{bmatrix} \quad (18)$$

In this expression, the vector on the left-hand side of the inequality can be denoted as x_{\min} , and the vector on the right-hand side is signified as x_{\max} .

The input variables have constrains $u \in \mathbb{U} \subseteq \mathbb{R}^{n_u}$, which are written as:

$$\begin{bmatrix} \beta_{\min} \\ T_{g,\min} \end{bmatrix} \leq \begin{bmatrix} \beta \\ T_g \end{bmatrix} \leq \begin{bmatrix} \beta_{\max} \\ T_{g,\text{rated}} \end{bmatrix} \quad (19)$$

Here, we make a representation that the vector on the left-hand side is u_{\min} , and the one on the right-hand side is u_{\max} .

The constraint on output power P_g is expressed through:

$$P_{g,\min} \leq P_g \leq P_{g,\text{rated}} \quad (20)$$

When the system operates in the constant power region, seeing that the large rotational inertia of the rotor in wind turbine and of the transmission system, it is hard for the controller to respond quickly, and some minor deviations beyond the hard constraints might occur. Thus, infeasible error lies in imposing strict hard constraints on the rotor speed and power. To address this issue, a soft constraint approach can be adopted, where some slight deviations beyond the hard constraints are permitted.

In this paper, it is assumed that the system rotor speed and output power can exceed the rated values 1.05 times to guarantee feasible solutions and better flexibility against wind speed variations. Thus the constrains can be modified as follows:

$$\begin{aligned} \omega_{g,\min} &\leq \omega_g \leq 1.05\omega_{g,\text{rated}} \\ \omega_{a,\min} &\leq \omega_a \leq 1.05\omega_{a,\text{rated}} \\ P_{g,\min} &\leq P_g \leq 1.05P_{g,\text{rated}} \end{aligned} \quad (21)$$

C. LYAPUNOV-BASED MPC DESIGN

In this section, LMPC will be employed in the wind power generation system to achieve better performance. Assuming that for all $x \in \mathbb{X}$, there exists a non-linear feedback control law $u = h(x) \in \mathbb{U}$. It satisfies the state constraints under the stability region w.r.t. control input u . The asymptotic stability of closed-loop system should be ensured at the nominal operating point. That is to say, according to the inverse Lyapunov theorem, the following inequalities hold for

the nominal closed-loop system [30], [31]:

$$\beta_1(|x|) \leq V(x) \leq \beta_2(|x|) \quad (22)$$

$$\frac{\partial V(x)}{\partial x} f(x, h(x), v) \leq -\beta_3(|x|) \quad (23)$$

$$\left| \frac{\partial V(x)}{\partial x} \right| \leq \beta_4(|x|) \quad (24)$$

where $\beta_i(\cdot)$, $i = 1, 2, 3, 4$ represents the \mathcal{K} -function, and is a continuous differentiable Lyapunov function.

In this paper, the region where the controlled system is stable under the input law $u = h(x)$ is defined as Ω . Particularly, $\Omega_\rho := \{x \in \mathbb{X} : V(x) \leq \rho\}$ indicates the Lyapunov-based stability region.

Lemma 1: If there exist positive constants $L_x, L_v, \bar{L}_x, \bar{L}_v$ and M such that the constraints are satisfied for all x and u , then the following inequalities hold:

$$|f(x, u, v) - f(\bar{x}, u, \bar{v})| \leq L_x |x - \bar{x}| + L_v |v - \bar{v}| \quad (25)$$

$$|f(x, u, v)| \leq M \quad (26)$$

$$\left| \frac{\partial V(x)}{\partial x} f(x, u, v) - \frac{\partial V(\bar{x})}{\partial x} f(\bar{x}, u, \bar{v}) \right| \leq \bar{L}_x |x - \bar{x}| + \bar{L}_v |v - \bar{v}| \quad (27)$$

Proof: In terms of the Lipschitz property of function f and the continuous differentiability of Lyapunov function $V(x)$, it is easy to derive (25)-(27). The details are omitted for brevity. The proof is completed. ■

To sum up, the optimization process of Lyapunov-based MPC can be demonstrated by the minimization problems below:

$$\min_{u \in \mathcal{S}(\Delta t)} \int_{t_k}^{t_k+N} \left(\|\tilde{y}(\tau) - y_s(\tau)\|_q^2 + \|\Delta u(\tau)\|_p^2 \right) d\tau \quad (28a)$$

$$s.t. \tilde{x}(t_k) = x(t_k) \quad (28b)$$

$$\dot{\tilde{x}}(t) = f(\tilde{x}(t), u(t), \tilde{v}(t)) \quad (28c)$$

$$\tilde{y}(t) = h(\tilde{x}(t), u(t)) \quad (28d)$$

$$u_{\min} \leq u(t) \leq u_{\max} \quad (28e)$$

$$x_{\min} \leq \tilde{x}(t) \leq x_{\max} \quad (28f)$$

$$P_{g,\min} \leq \tilde{P}_g(t) \leq P_{g,\text{rated}} \quad (28f)$$

$$\frac{\partial V(x(t_k))}{\partial x} f(x(t_k), u(t_k), v(t_k)) \leq \quad (28g)$$

$$\frac{\partial V(x(t_k))}{\partial x} f(x(t_k), h(x(t_k)), v(t_k)) \quad (28h)$$

In this optimization problem, the objective function $J(\tilde{y}, u) = \|\tilde{y} - y_s\|_q^2 + \|\Delta u\|_p^2$ is introduced to be minimized; $\mathcal{S}(\Delta t)$ represents a continuous piecewise function family with sampling period Δt ; t_k is used as the current time; $\tilde{x}(t_k)$ is the predicted states at time k ; \tilde{v} is the predicted wind speed; N is the prediction horizon. The optimization problem is a formulation over the whole prediction horizon. \tilde{y} denotes the predicted output; y_s represents the desired target value for the output variables based on the current states and wind speed; Δu indicates the change in inputs, i.e., the difference between the current input and the one at the previous sampling time.

q and p are positive definite matrices with $q = \text{diag}\{q_1, q_2\}$, $p = \text{diag}\{p_1, p_2\}$. These matrices are set to weighing the consideration in the control problem. It means, larger values of q_1 and q_2 emphasize the distance between output values and target values, while larger values of p_1 and p_2 stress the input variations.

In a word, the optimization (28) can be described as a process of searching a sequence of inputs within a specific sampling period from the current time k . Not only are all the constraints satisfied, the objective function is also minimized for the optimal performance. The solution will be updated as time goes on.

The above objective function is rewritten as follows:

$$J(\tilde{y}, u) = \|P_g - P_g^*\|_{q_1}^2 + \|\omega_g - \omega_g^*\|_{q_2}^2 + \|\Delta u_1\|_{p_1}^2 + \|\Delta u_2\|_{p_2}^2 \quad (29)$$

In the equation, the first part of objective function represents the difference between output power and target values, as well as that between generator speed and target. Evidently, if the outputs are equal to the target ones, the difference is zero. The second part of the objective function suggests the weighted sum of the changes in inputs. It takes the impact of input variations on the system's behavior into account. By modifying the weighting matrices q and p , the sensitivity of optimization process to different inputs/outputs can be adjusted.

Based on the LMPC optimization strategy mentioned above, in the maximum wind energy capture region, we use the optimal tip speed ratio method to drive the outputs to corresponding targets. In addition, it is a need to maintain the generator speed and output power at their rated values, which means the desired targets should be fixed as the rated values. The details are shown in the follow-up:

$$\omega_g^* = \begin{cases} \frac{\lambda_{opt} v}{R} & v \leq v_{\text{rated}} \\ \omega_{g,\text{rated}} & v > v_{\text{rated}} \end{cases} \quad (30)$$

$$P_g^* = \begin{cases} \frac{1}{2} \eta \rho \pi R^2 v^3 C_{p,\max} & v \leq v_{\text{rated}} \\ P_{g,\text{rated}} & v > v_{\text{rated}} \end{cases} \quad (31)$$

Remark 1: The optimization problem (28) involves finding the input values that minimize the objective function subject to certain constraints. We define constraints that control the inputs and states to ensure that the system satisfies the physical and performance constraints in operation. An objective function which measures the performance of the system is derived. The goal is to minimize the objective function by optimizing the control inputs. To solve this optimization problem, `fmincon` function in MATLAB is used to find the optimal control input. The optimization problem (28) is a nonlinear constrained optimization algorithm that finds the minimum value of the objective function with constraints. The first value of this input sequence is used as the input for the next step and repeat this minimization process. The specific design steps of LMPC are shown in Algorithm 1.

Algorithm 1 (Lyapunov-Based MPC Algorithm)

Offline. Accurately model the state-space equations of the wind power generation system, define the constraints for the system optimization process, determine the initial states x_0 and initial input u_0 , and define the system’s weight parameters q and q .

Online.

- 1: Obtain the current wind speed and choose different optimization goals and loss functions based on the current wind speed magnitude;
- 2: Based on the optimization goal from step 1, find the input $u^*(t_k), u^*(t_{k+1}), \dots, u^*(t_{k+N-1})$ that minimizes the loss function within the predicted time domain, while satisfying the constraints;
- 3: Take the first input $u^*(t_k)$ from step 2 as the current input applied to the system and obtain the updated state variables;
- 4: Set $k = k + 1$, return to step 1, and repeat the process until the program ends.

D. STABILITY ANALYSIS

The proposed LMPC algorithm regulates the system through solving the constrained optimization problem (28). It is necessary to prove the Lyapunov function’s decremental property for the closed-loop stability analysis. Some sufficient conditions for stability are conducted.

At first, we define a scalar:

$$\rho_{\min} = \max \{V(x(t + t_s)) : V(x(t)) \leq \rho_s\} \quad (32)$$

where ρ_s is a scalar smaller than ρ . Therefore, ρ_{\min} represents the maximum value of $V(x(t + t_s))$ that can taken the next sampling time when $V(x(t))$ is less than ρ .

Next, a set of sufficient conditions for the system stability are concluded as follows for our LMPC scheme.

Theorem 1: Assume that the inequalities (22)-(24) are fulfilled. For the closed-loop system (15), controlled by optimization (28), if $x(t_0) \in \Omega_\rho$ and there exist constants $\varepsilon > 0, \rho > \rho_s > 0$ such that the following conditions hold:

$$-\beta_3 \left(\beta_3^{-1}(\rho_s) \right) + \bar{L}_x M t_s + \bar{L}_v \varphi \leq \frac{\varepsilon}{t_s} \quad (33)$$

where φ is the upper bound of wind speed variation within the sampling period. Then, there exists $\rho > \rho_{\min} > 0$, for all $t \geq t_0$, guarantee the system states $x(t)$ remaining within the stable region $\Omega_{\rho_{\min}}$.

Proof: Considering the closed-loop system at time $t \in [t_k, t_{k+1})$, the time-derivative of Lyapunov function can be calculated as follows:

$$\dot{V}(x(t)) = \frac{\partial V(x(t))}{\partial x} f(x(t), u(t), v(t)) \quad (34)$$

Based on the constraints (28g), we can extend (34) to the following inequality:

$$\begin{aligned} \dot{V}(x(t)) \leq & \frac{\partial V(x(t))}{\partial x} f(x(t), u(t), v(t)) \\ & - \frac{\partial V(x(t_k))}{\partial x} f(x(t_k), u(t_k), v(t_k)) \\ & + \frac{\partial V(x(t_k))}{\partial x} f(x(t_k), h(x(t_k)), v(t_k)) \end{aligned} \quad (35)$$

Then by virtue of (27), (35) is rewritten as:

$$\begin{aligned} \dot{V}(x(t)) \leq & \frac{\partial V(x(t_k))}{\partial x} f(x(t_k), h(x(t_k)), v(t_k)) \\ & + \bar{L}_x |x(t) - x(t_k)| + \bar{L}_v |v(t) - v(t_k)| \end{aligned} \quad (36)$$

Due to (26) and the continuity of $x(t)$, it follows that within one sampling period:

$$|x(t) - x(t_k)| \leq M t_s \quad (37)$$

From (23), it can be derived that:

$$\frac{\partial V(x(t_k))}{\partial x} f(x(t_k), h(x(t_k)), v(t_k)) \leq -\beta_3 \left(\beta_3^{-1}(\rho_s) \right) \quad (38)$$

By substituting (37) and (38) into (36), we obtain:

$$\dot{V}(x(t)) \leq -\beta_3 \left(\beta_3^{-1}(\rho_s) \right) + \bar{L}_x M t_s + \bar{L}_v \varphi \quad (39)$$

If (33) is satisfied, then there exists a $\varepsilon > 0$ such that the following inequalities hold:

$$\dot{V}(x(t)) \leq -\frac{\varepsilon}{t_s} \quad (40)$$

It shows that when $t \in [t_k, t_{k+1})$, the function $V(x(t))$ remains decreasing. Integrating this inequality from time t_k to time t_{k+1} , it yields:

$$V(x(t_{k+1})) \leq V(x(t_k)) - \varepsilon \quad (41)$$

Hence, it can be concluded that if $x(t_k) \in \Omega_\rho$, then all states $x(t)$ remain in the stable region Ω_ρ at time $t > t_k$. As well, the states $x(t)$ will gradually converge to $\Omega_{\rho_{\min}}$ within a finite number of sampling times, and stay at this stable region all the future time.

IV. SIMULATION EXPERIMENTS

A. WIND POWER GENERATION SYSTEM

In this section, a 5MW wind turbine system, constructed by the National Renewable Energy Laboratory (NREL) for offshore system development [28], is taken to validate the proposed LMPC algorithm. The specific parameters for the simulation stem from [28] and are given in TABLE 1. Besides, the soft constraints presented in (21) are followed, with an upper limit increase of 5% applied to ω_a, ω_g and P_g additionally.

Note that, in our research, all the simulation experiments are conducted using the same prediction horizon and sampling time, namely $N = 10, t_s = 0.05s$.

TABLE 1. Parameters of a 5MW wind power generation system.

Parameter symbols	Values and Units
η_g	94.4%
N_g	97
λ_{opt}	8.1rad
J_a	$1.2 \times 10^7 kg \cdot m^2$
J_g	$543.11kg \cdot m^2$
K_s	$8.676 \times 10^8 N \cdot m/rad$
D_s	$6.215 \times 10^6 N \cdot m/rad$
ρ	$1.225kg/m^3$
R_a	63m
v_{rated}	11.4m/s
$C_{p,max}$	0.48
$\omega_{a,min}$	0.3595rad/s
$\omega_{a,rated}$	1.2671rad/s
$\omega_{g,min}$	0rad/s
$\omega_{g,rated}$	122.9096rad/s
$T_{g,min}$	0N · m
$T_{g,rated}$	43095N · m
θ_{min}	0rad
θ_{max}	0.01rad
$P_{g,rated}$	5×10^6
β_{min}	0°
β_{max}	90°

B. LMPC SIMULATION RESULTS UNDER LOW WIND SPEED

The proposed wind speed model in Section II is considered in the simulation. At the low wind speed stage, the mean wind speed is described by a step function. It starts at 7.5m/s (time = 0s), increases to 8m/s (time = 5s), and finally reaches 9m/s (time = 20s). The turbulent wind speed v_r is modeled through truncated Gaussian distribution, with $\mu = 0$, $\sigma = 0.02$ and truncation amplitude $v_c = 0.1$. It is randomly re-generated every 0.5s, as shown in FIGURE 6.

As we can see, wind speed varies at different times depending on the changes in average wind speed and turbulent wind speed. Since the wind speed is not measurable, the average wind speed is used for controller design purpose and the changes of the wind speed is treated as disturbances.

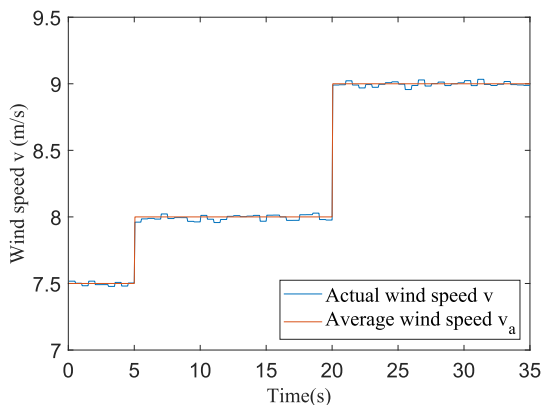


FIGURE 6. Wind speed used in the simulation for low wind conditions.

Under the low wind speed, the designed control aims to gain the maximum wind energy. The optimal tip speed ratio method is utilized, which maintain the pitch angle close to 0° and propel the tip speed toward the optimal value. To investigate the influence of different weighting coefficients, the control parameters of objective function below are selected in the simulations: output weight as $diag\{1 \times 10^{-3}, q_2\}$, and input weight $diag\{1 \times 10^8, 50\}$. The value q_2 is taken from 4×10^7 , 5×10^7 and 6×10^7 . The simulation results are depicted in FIGURE 7.

Some conclusions can be drawn from the result plots. At the low wind speed stage, the control objective is to keep the system stay in the maximum wind energy capture region, and the system disturbed by turbulent wind can be effectively controlled. It adjusts the states and outputs to the target values within 5s to deal with the variations of mean wind speed. Furthermore, fast response is acquired for the adverse effect of turbulent wind. Thus there are slight changes take places on the states and output power when turbulent wind changes. Moreover, FIGURE 7 reveals the performance has been quite affected by the weighting parameter q_2 , which represent the priority of adjusting the generator speed to the target value. Obviously, as q_2 increases, the rotational speed in generator and wind turbine are both converge quicker to their target values, whereas it also results in higher fluctuations on variables such as generator torque, output power and twist angle.

TABLE 2. Running time and average loss of different q_2 under low wind speed.

Value of q_2	Running time t/s	Average loss \bar{J}
4×10^7	1.7408×10^3	2.9241×10^8
5×10^7	1.7211×10^3	3.1171×10^8
6×10^7	1.7331×10^3	3.3136×10^8

Under low wind speed and different q_2 , TABLE 2 presents two kinds of metrics to illustrate the performance of controlled wind power generation system. It is shown that there exists little difference on the running time. Under low wind speed, a total of 900 iterations were conducted, with an average time of approximately 1.9 seconds per step for different weights. From the perspective of single-step computational complexity, this speed needs improvement. However, in terms of average loss, it increase to a certain extent with the growth of q_2 . Additionally, it is also related to the increasing fluctuation amplitudes of some state variables and output power, as mentioned above.

To demonstrate the effectiveness of LMPC compared to regular MPC [32], we conducted simulation comparing the two methods, as shown in FIGURE 8. To ensure the fairness of the method comparison, we have to make the consistent of the system models and guarantee that both LMPC and MPC achieve their best performance. For the

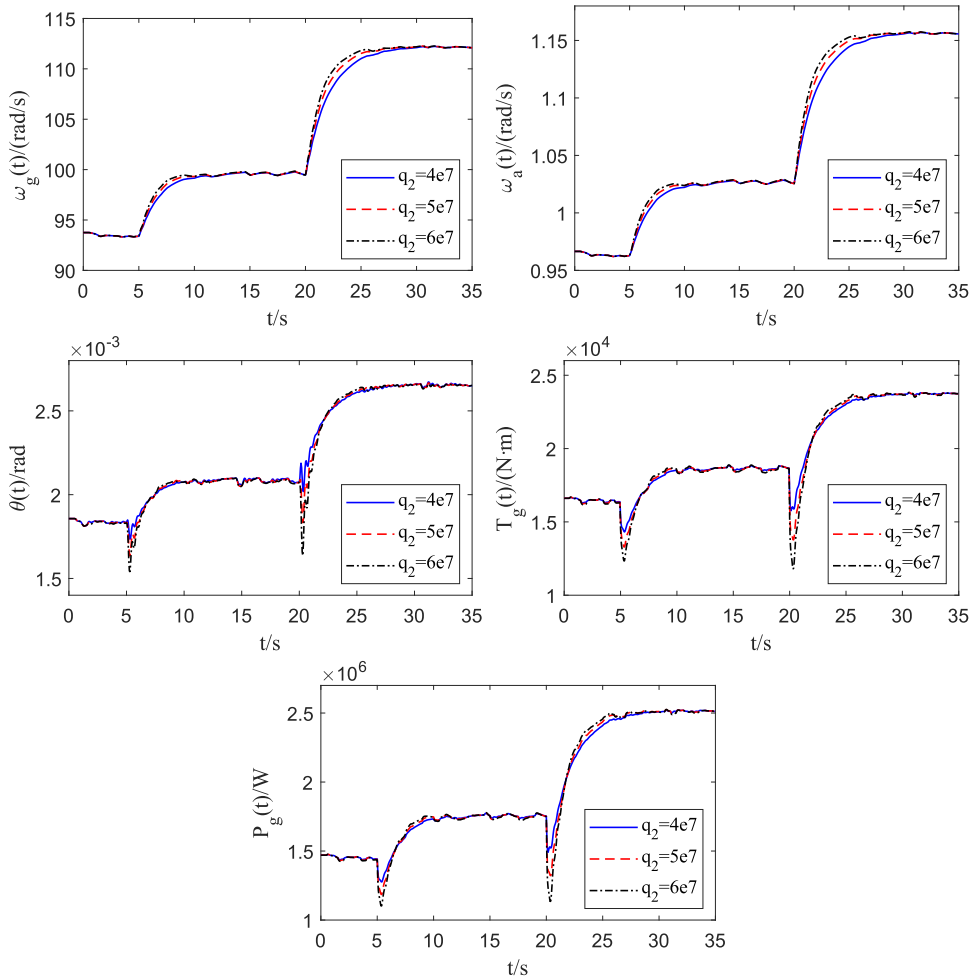


FIGURE 7. Simulation results of different q_2 under low wind speed.

consistent of the system models, both LMPC and MPC methods utilize the 5 MW wind generation system with same parameters as shown in TABLE 1. Additionally, external disturbances during the system’s operation, represented in the article by the turbulent wind speed component, are identical for both LMPC and MPC methods, as illustrated in FIGURE 6. To guarantee both LMPC and MPC achieve their best performance, we do fine-tune on the selections of both LMPC and MPC methods. Firstly, the control costs are selected the same. Secondly, the best performances are obtained by fine-tuning the prediction time horizon N , the weighting matrix on outputs and inputs (respectively represented by q and p). Finally, the LMPC and MPC compared in a same figure to show the control performance.

From the figure, it is evident that at the low wind speed stage, LMPC provides a more stable control for the state variables, with smaller fluctuations compared to MPC, and it reaches the target values more quickly. However, this comes at a cost, as the input fluctuations in LMPC are greater than in MPC. Through the simulation comparison of

these two methods, we observed that the proposed approach exhibits characteristics of being faster and more stable compared to regular MPC at the low wind speed stage. This validates the effectiveness of the proposed method in simulation.

C. LMPC SIMULATION RESULTS UNDER HIGH WIND SPEED

At the high wind speed stage, the mean wind speed v_a starts from 20m/s (time = 0s), decreases to 18m/s (time = 5s), and finally reaches 16m/s (time = 15s). The random turbulent wind speed v_r is obtained through the same model as low wind speed stage. The parameters are $\mu = 0$, $\sigma = 0.02$ and truncation amplitude is $v_c = 0.1$. Similarly, the turbulent wind is re-evaluated every 0.5s. FIGURE 9 gives the wind speed used in the simulation overall.

Based on the LMPC optimization strategy, at the high wind speed stage, the maintenance in rated output power is our control objective. In the simulation, the output weight is denoted as $[q_1, q_2] = [1 \times 10^{-4}, q_2]$, and the input weight

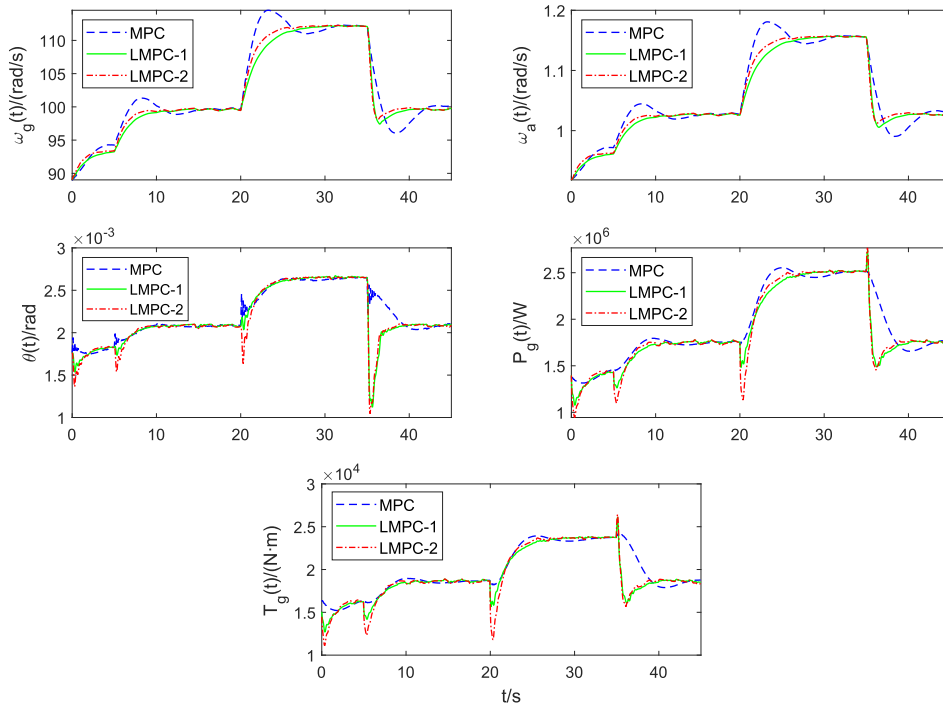


FIGURE 8. Comparison between LMPC and Regular MPC under Low Wind Speed.

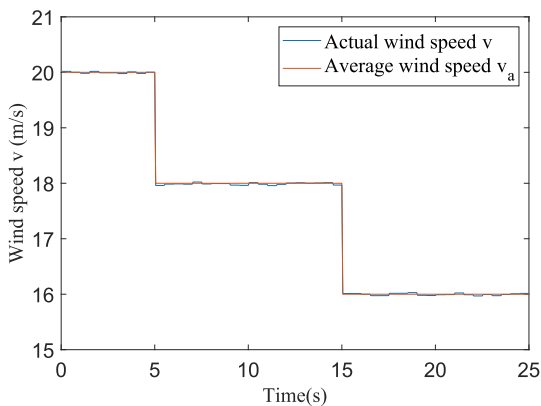


FIGURE 9. Wind speed used in the simulation for high wind conditions.

as $[p_1, p_2] = [1 \times 10^8, 50]$. Also, different weighting values of q_2 are chosen from 1×10^8 , 2×10^8 and 3×10^8 .

FIGURE 10 draws the system responses under high wind speed. In this case, when the system disturbed by turbulent wind, LMPC strategy enables the output power to stay at the rated value. What's more, the settling time is smaller than that spent under low wind, also indicating the fact that all the responses tend to the targets within 2s. It is plain to see a faster convergence at high wind speed stage. As well, the turbulent wind brings about some slight changes of system states and output power.

In addition, it yields the differences on performance, since q_2 varies. The rotational speed in generator and wind

TABLE 3. Running time and average loss of different q_2 under high wind speed.

Value of q_2	Running time t/s	Average loss \bar{J}
1×10^8	1.1049×10^3	4.1983×10^6
2×10^8	1.1244×10^3	4.5792×10^6
3×10^8	1.1323×10^3	4.8161×10^6

turbine have a quicker trend to their target values and lower fluctuating magnitude as q_2 increases, whereas some faint waves appear at the generator torque, output power and twist angle. The comparison of performance metrics is summarized in TABLE 3. It can be observed that, for different q_2 , the spent running time remains relatively consistent with a total of 500 iterations and an average time of approximately 2.2 seconds per step for different weights. However, the average loss grows as q_2 increases. It can be attributed the facts that the numerical rise caused by increasing q_2 , and the higher fluctuating magnitude of system states.

FIGURE 11 shows the comparison between LMPC and Regular MPC under high wind speed. Similar conclusions to those obtained under low wind speed can be drawn. Under high wind speed, LMPC demonstrates more stable control over the state variables and can reach the target values more rapidly. Meanwhile, the input fluctuation amplitude of LMPC is greater compared to MPC. This provides evidence that the proposed LMPC exhibits faster and more stable characteristics compared to regular MPC under high wind speed.

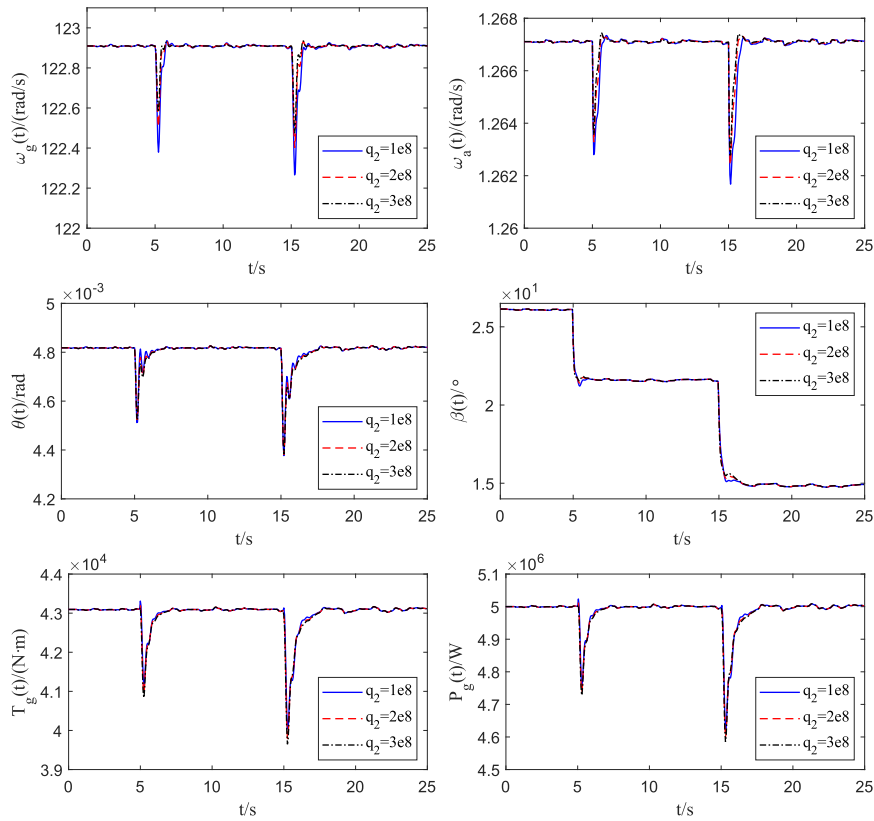


FIGURE 10. Simulation results of different q_2 under high wind speed.

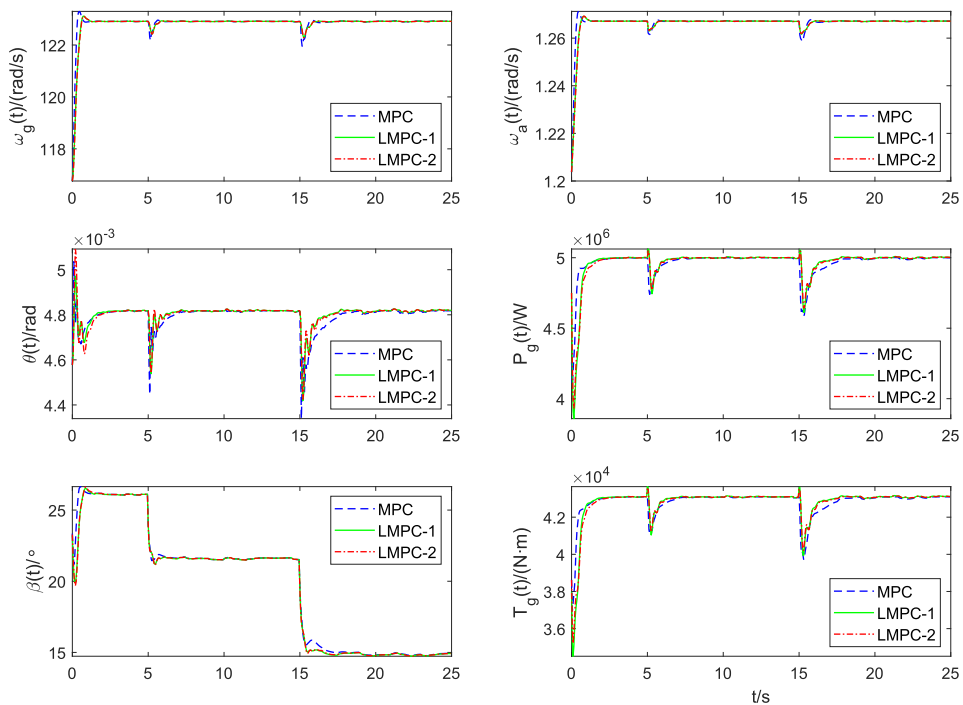


FIGURE 11. Comparison between LMPC and Regular MPC under High Wind Speed.

V. CONCLUSION

This work proposes a Lyapunov-based MPC framework, which is utilized to address the nonlinear control issues in wind power generation systems, and ensure the system operation subject to specific constraints. Simulation experiments on a 5MW wind power generation system is given to validate the feasibility and effectiveness of the designed LMPC strategy under low/high wind speed. The results demonstrate that the proposed Lyapunov MPC method can achieve great robust stability and control performance on the fast response to step-changing mean wind speed and the resistance against stochastic turbulent wind. The proposed method also has some shortcomings, even it demonstrates some improvement in handling complex nonlinear systems and external perturbations. For example, in real applications, model uncertainties, time delays and stochastic factors are unavoidable under network environment. The proposed LMPC method fails to consider these factors and cannot deal with these complicate circumstances. Thus, how to incorporate these model uncertainties and network induced elements remains challenging problems for our future research.

ACKNOWLEDGMENT

The authors would like to thank the Editor and the anonymous reviewers for their valuable suggestions and comments.

REFERENCES

- [1] M. Talaat, M. A. Farahat, and M. H. Elkholy, "Renewable power integration: Experimental and simulation study to investigate the ability of integrating wave, solar and wind energies," *Energy*, vol. 170, pp. 668–682, Mar. 2019.
- [2] A. F. Tazay, A. M. A. Ibrahim, O. Noureldeen, and I. Hamdan, "Modeling, control, and performance evaluation of grid-tied hybrid PV/wind power generation system: Case study of Gabel El-Zeit region, Egypt," *IEEE Access*, vol. 8, pp. 96528–96542, 2020.
- [3] S. Behera, S. Sahoo, and B. B. Pati, "A review on optimization algorithms and application to wind energy integration to grid," *Renew. Sustain. Energy Rev.*, vol. 48, pp. 214–227, Aug. 2015.
- [4] X. Liu, L. Feng, and X. Kong, "A comparative study of robust MPC and stochastic MPC of wind power generation system," *Energies*, vol. 15, no. 13, p. 4814, Jun. 2022.
- [5] X. Kong, X. Wang, M. A. Abdelbaky, X. Liu, and K. Y. Lee, "Nonlinear MPC for DFIG-based wind power generation under unbalanced grid conditions," *Int. J. Electr. Power Energy Syst.*, vol. 134, Jan. 2022, Art. no. 107416.
- [6] O. P. Mahela, N. Gupta, M. Khosravy, and N. Patel, "Comprehensive overview of low voltage ride through methods of grid integrated wind generator," *IEEE Access*, vol. 7, pp. 99299–99326, 2019.
- [7] H. Chojaa, A. Derouich, O. Zamzoum, S. Mahfoud, M. Taoussi, H. Albalawi, H. Benbouhenni, and M. I. Mosaad, "A novel DPC approach for DFIG-based variable speed wind power systems using DSpace," *IEEE Access*, vol. 11, pp. 9493–9510, 2023.
- [8] L. Zhang, B. Wang, Y. Li, and Y. Tang, "Distributed stochastic model predictive control for cyber-physical systems with multiple state delays and probabilistic saturation constraints," *Automatica*, vol. 129, Jul. 2021, Art. no. 109574.
- [9] D. Cui and H. Li, "Dual self-triggered model-predictive control for nonlinear cyber-physical systems," *IEEE Trans. Syst., Man, Cybern. Syst.*, vol. 52, no. 6, pp. 3442–3452, Jun. 2022.
- [10] M. Bujarbaruah, U. Rosolia, Y. R. Stürz, X. Zhang, and F. Borrelli, "Robust MPC for LPV systems via a novel optimization-based constraint tightening," *Automatica*, vol. 143, Sep. 2022, Art. no. 110459.
- [11] Z. Sun, L. Dai, K. Liu, Y. Xia, and K. H. Johansson, "Robust MPC for tracking constrained unicycle robots with additive disturbances," *Automatica*, vol. 90, pp. 172–184, Apr. 2018.
- [12] J. Hu and B. Ding, "Output feedback robust MPC for linear systems with norm-bounded model uncertainty and disturbance," *Automatica*, vol. 108, Oct. 2019, Art. no. 108489.
- [13] R. Heydari and M. Farrokhi, "Robust tube-based model predictive control of LPV systems subject to adjustable additive disturbance set," *Automatica*, vol. 129, Jul. 2021, Art. no. 109672.
- [14] Y. Song, Z. Wang, D. Ding, and G. Wei, "Robust H_2/H_∞ model predictive control for linear systems with polytopic uncertainties under weighted MEF-TOD protocol," *IEEE Trans. Syst., Man, Cybern. Syst.*, vol. 49, no. 7, pp. 1470–1481, Jul. 2019.
- [15] L. Zhang, B. Wang, Y. Zheng, A. Zemouche, X. Zhao, and C. Shen, "Robust packetized MPC for networked systems subject to packet dropouts and input saturation with quantized feedback," *IEEE Trans. Cybern.*, vol. 53, no. 11, pp. 6987–6997, 2023.
- [16] L. Zhang, J. Wang, and C. Li, "Distributed model predictive control for polytopic uncertain systems subject to actuator saturation," *J. Process Control*, vol. 23, no. 8, pp. 1075–1089, Sep. 2013.
- [17] X. Kong, X. Liu, L. Ma, and K. Y. Lee, "Hierarchical distributed model predictive control of standalone wind/solar/battery power system," *IEEE Trans. Syst., Man, Cybern. Syst.*, vol. 49, no. 8, pp. 1570–1581, Aug. 2019.
- [18] J. Liu, Q. Yao, and Y. Hu, "Model predictive control for load frequency of hybrid power system with wind power and thermal power," *Energy*, vol. 172, pp. 555–565, Apr. 2019.
- [19] M. Farbood, M. Shasadeghi, T. Niknam, and B. Safarinejadian, "Fuzzy Lyapunov-based model predictive sliding-mode control of nonlinear systems: An ellipsoid recursive feasibility approach," *IEEE Trans. Fuzzy Syst.*, vol. 30, no. 6, pp. 1929–1938, Jun. 2022.
- [20] M. Farbood, M. Veysi, M. Shasadeghi, A. Izadian, T. Niknam, and J. Aghaei, "Robustness improvement of computationally efficient cooperative fuzzy model predictive-integral sliding mode control of nonlinear systems," *IEEE Access*, vol. 9, pp. 147874–147887, 2021.
- [21] M. Farbood, M. Shasadeghi, T. Niknam, B. Safarinejadian, and A. Izadian, "Cooperative H_∞ robust move blocking fuzzy model predictive control of nonlinear systems," *IEEE Trans. Syst., Man, Cybern. Syst.*, vol. 53, no. 12, pp. 7707–7718, Dec. 2023.
- [22] D. M. de la Pena and P. D. Christofides, "Lyapunov-based model predictive control of nonlinear systems subject to data losses," *IEEE Trans. Autom. Control*, vol. 53, no. 9, pp. 2076–2089, Oct. 2008.
- [23] M. Mahmood and P. Mhaskar, "Lyapunov-based model predictive control of stochastic nonlinear systems," *Automatica*, vol. 48, no. 9, pp. 2271–2276, Sep. 2012.
- [24] H. Makhmreh, M. Trabelsi, O. Kükrer, and H. Abu-Rub, "A Lyapunov-based model predictive control design with reduced sensors for a PUC7 rectifier," *IEEE Trans. Ind. Electron.*, vol. 68, no. 2, pp. 1139–1147, Feb. 2021.
- [25] C. N. Manh, N. T. Nguyen, N. B. Duy, and T. L. Nguyen, "Adaptive fuzzy Lyapunov-based model predictive control for parallel platform driving simulators," *Trans. Inst. Meas. Control*, vol. 45, no. 5, pp. 838–852, Mar. 2023.
- [26] B. Babaghorbani, M. T. Beheshti, and H. A. Talebi, "A Lyapunov-based model predictive control strategy in a permanent magnet synchronous generator wind turbine," *Int. J. Electr. Power Energy Syst.*, vol. 130, Sep. 2021, Art. no. 106972.
- [27] W.-M. Lin and C.-M. Hong, "Intelligent approach to maximum power point tracking control strategy for variable-speed wind turbine generation system," *Energy*, vol. 35, no. 6, pp. 2440–2447, Jun. 2010.
- [28] J. Jonkman, S. Butterfield, W. Musial, and G. Scott, "Definition of a 5-MW reference wind turbine for offshore system development," Nat. Renew. Energy Lab., Golden, CO, USA, Tech. Rep. NREL/TP-500-38060, 2009.
- [29] S. Liu and J. Liu, "Distributed Lyapunov-based model predictive control with neighbor-to-neighbor communication," *AIChE J.*, vol. 60, no. 12, pp. 4124–4133, Dec. 2014.
- [30] R. Wang and J. Bao, "A differential Lyapunov-based tube MPC approach for continuous-time nonlinear processes," *J. Process Control*, vol. 83, pp. 155–163, Nov. 2019.
- [31] P. Gong, Z. Yan, W. Zhang, and J. Tang, "Lyapunov-based model predictive control trajectory tracking for an autonomous underwater vehicle with external disturbances," *Ocean Eng.*, vol. 232, Jul. 2021, Art. no. 109010.
- [32] J. Yang, X. Sun, K. Liao, Z. He, and L. Cai, "Model predictive control-based load frequency control for power systems with wind-turbine generators," *IET Renew. Power Gener.*, vol. 13, no. 15, pp. 2871–2879, 2019.



JINMAN LUO received the master's degree from the School of Computer Science, South China University of Technology, Guangzhou, China, in 2011. Currently, he is a Leading Technical Expert with the Information Center, Dongguan Power Supply Bureau of Guangdong Power Grid Corporation, China. His main research directions are distributed energy cluster control, data center energy collaborative optimization, and data analysis systems.



SIQI YE received the bachelor's degree in management from the School of Computer and Artificial Intelligence, Southwest University of Finance and Economics, Chengdu, China, in 2019, and the master's degree in computer and science from The University of Hong Kong, China, in 2021. He is currently a Senior Operator with the Data Application Class, Information Center, Dongguan Power Supply Bureau of Guangdong Power Grid Corporation, China. His main research directions are multimodal image retrieval, dynamic graph neural networks, and multi energy collaborative optimization.



YUQING LI received the bachelor's degree in law from the School of Law, South China University of Technology, Guangzhou, China, in 2010, and the master's degree in law from Sun Yat-sen University, Guangzhou, in 2012. She is currently responsible for business supervision with the Supply Chain Center, Dongguan Power Supply Bureau of Guangdong Power Grid Corporation, China. Her main research directions are intelligent supervision and supply chain intelligence.



RUIJUE FENG received the master's degree in electrical engineering and automation from the School of Engineering, South China Agricultural University, Guangzhou, China, in 2012. Currently, she is the Deputy Director and an Associate Professor with the Electrical Teaching and Research Office, College of Electrical Engineering, Guangzhou City University of Technology. Her main research direction is information security technology research.



PIAO LIU received the master's degree in power system and automation from the South China University of Technology, in 2019. Since 2019, he has been with Dongguan Power Supply Bureau of Guangdong Power Grid Corporation. His main research interests include digital power grid communication technology, power system fault analysis and relay protection, and the application of artificial intelligence technology in power systems.



JINYANG WANG received the bachelor's degree in engineering from the School of Electrical and Information Engineering, Changsha University of Technology, in 2021. He is currently pursuing the master's degree with the South China University of Technology. His main research direction includes cable line load regulation and optimization.